Assessment of aerodynamic behaviour of the NACA 64A212 airfoil on the context of computational fluid dynamics

RMPS Bandara[1] and JI Abeygoonewardena [2]

[1]Department of Mechanical Engineering, [2]Department of Aeronautical Engineering, Faculty of Engineering, General Sir John Kotelawala Defence University, Sri Lanka

[1] bandara@kdu.ac.lk, [2] jabeygoonewardene@kdu.ac.lk

Abstract— *A comprehensive understanding of an aircraft's fluid and flight dynamics cannot be understated from both an engineering and aircraft handling perspective. In this context, availability of such descriptive information, especially in the case of trainer aircraft, will deliver profitable results for both students and teachers. This research examines the behaviour of an aircraft having a wing tip designed with the NACA 64A212 airfoil. Detailed information regarding the aerodynamic behaviour of the wing has not been disclosed by the aircraft manufacturer to relevant stakeholders. Due to the complexity of flow physics involved during different regimes of the flight envelope, analytical fluid dynamic modelling does not render completely accurate results for the appraisal of the vehicle aerodynamic behaviour.*

The present work is involved with the assessment of aerodynamic behaviour of the NACA 64A212 airfoil through Computational Fluid Dynamics (CFD) methodology. The geometry of the airfoil is created using a solid modelling software and a commercial CFD tool models the flow physics involved. A generic lift curve and drag polar is developed to represent flows of reasonable Reynolds number that the vehicle would experience in actual flight. The results provide new insights into the behaviour of the airfoil, thus enabling means of enhancing handling qualities of the aircraft.

Keywords— **Aerodynamics, Airfoil, CFD**

I. INTRODUCTION

The relationship among fundamental flow properties are described through Navier-Stokes Equations, as shown below in the three dimensional unsteady form.

Continuity: $$\frac{\partial \rho}{\partial t}+\frac{\partial(\rho u)}{\partial x}+\frac{\partial(\rho v)}{\partial y}+\frac{\partial(\rho w)}{\partial z}=0$$

X-Momentum:

$$\frac{\partial(\rho u)}{\partial t}+\frac{\partial\left(\rho u^{2}\right)}{\partial x}+\frac{\partial(\rho u v)}{\partial y}+\frac{\partial(\rho u w)}{\partial z}$$
$$=-\frac{\partial p}{\partial x}+\frac{1}{\mathrm{Re}_{f}}\left[\frac{\partial \tau_{xx}}{\partial x}+\frac{\partial \tau_{xy}}{\partial y}+\frac{\partial \tau_{xz}}{\partial z}\right]$$

Y-Momentum:

$$\frac{\partial(\rho v)}{\partial t}+\frac{\partial(\rho u v)}{\partial x}+\frac{\partial\left(\rho v^{2}\right)}{\partial y}+\frac{\partial(\rho v w)}{\partial z}$$
$$=-\frac{\partial p}{\partial y}+\frac{1}{\mathrm{Re}_{f}}\left[\frac{\partial \tau_{xy}}{\partial x}+\frac{\partial \tau_{yy}}{\partial y}+\frac{\partial \tau_{yz}}{\partial z}\right]$$

Z-Momentum:

$$\frac{\partial(\rho w)}{\partial t}+\frac{\partial(\rho u w)}{\partial x}+\frac{\partial(\rho v w)}{\partial y}+\frac{\partial\left(\rho w^{2}\right)}{\partial z}$$
$$=-\frac{\partial p}{\partial z}+\frac{1}{\mathrm{Re}_{f}}\left[\frac{\partial \tau_{xz}}{\partial x}+\frac{\partial \tau_{yz}}{\partial y}+\frac{\partial \tau_{zz}}{\partial z}\right]$$

Energy:

$$\frac{\partial\left(E_{T}\right)}{\partial t}+\frac{\partial\left(u E_{T}\right)}{\partial x}+\frac{\partial\left(v E_{T}\right)}{\partial y}+\frac{\partial\left(w E_{T}\right)}{\partial z}$$
$$=-\frac{\partial(u p)}{\partial x}-\frac{\partial(v p)}{\partial y}-\frac{\partial(w p)}{\partial z}-\frac{1}{\mathrm{Re}_{f}\,\mathrm{Pr}_{f}}\left[\frac{\partial q_{x}}{\partial x}+\frac{\partial q_{y}}{\partial y}+\frac{\partial q_{z}}{\partial z}\right]$$
$$+\frac{1}{\mathrm{Re}_{f}}[\frac{\partial}{\partial x}\left(u \tau_{xx}+v \tau_{xy}+w \tau_{xz}\right)$$
$$+\frac{\partial}{\partial y}\left(u \tau_{xy}+v \tau_{yy}+w \tau_{yz}\right)+\frac{\partial}{\partial z}\left(u \tau_{xz}+v \tau_{yz}+w \tau_{zz}\right)]$$

These equations consist of a time-dependent continuity equation for the conservation, three time dependent conservation of momentum equations and a time-dependent conservation of energy equation. The spatial coordinates of the domain, denoted by **x**, **y** and **z**, as well as the time, t, are the four independent variables. The six dependent variables include pressure, density, temperature and the three components of the velocity vector; **u**, **v**, and **w** in the **x**, **y** and **z** directions respectively. All dependent variables are functions of all independent variables, thus resulting in a set of partial differential equations.

The net aerodynamic force over a body is purely due to the shear stress and pressure distribution over the body acting in parallel and normal at any given point on the surface. If p and τ are the local pressure and shear stress at a point, then the resultant aerodynamic force **R** on the body can be written as

$$R=-\iint_{S} pn dS+\iint_{S} \tau k dS$$

By definition, the perpendicular component of R to the free stream is the lift L, and the parallel component to the free stream is drag, D. The effect of the two forces acting on the body gives rise to a moment, which is conventionally calculated around the quarter chord of an airfoil. Intuitively, these fundamental forces and moments are directly dependent on free stream velocity; $V_{\infty}V_{\infty}$, surface area, S, angle of attack, α, coefficient of viscosity,

μ, and compressibility of the medium, aa:

$$L = L(\rho_\infty, V_\infty, S, \alpha, \mu_\infty, a_\infty)$$

$$D = D(\rho_\infty, V_\infty, S, \alpha, \mu_\infty, a_\infty)$$

$$M = M(\rho_\infty, V_\infty, S, \alpha, \mu_\infty, a_\infty)$$

Lift, drag and moment coefficients denoted by C_L, C_D and C_M *are* related to the dynamic pressure q_∞ as follows:

$$C_L = \frac{L}{q_\infty S}$$

$$C_D = \frac{D}{q_\infty S}$$

$$C_M = \frac{M}{q_\infty S c}$$

where c is the characteristic length.

Force and Moment coefficients are more fundamental descriptions of the aerodynamic characteristics of a body than the actual force and moments themselves. While the aerodynamic force and moment on a body vary depending on ambient dynamic pressure, surface area and angle of attack of the body, as well as the coefficient of viscosity and compressibility of the medium; the aerodynamic coefficients are direct representations of angle of attack, Reynolds number and Mach number.

$$C_L = f_1(\alpha, Re, M_\infty)$$

$$C_D = f_2(\alpha, Re, M_\infty)$$

$$C_M = f_3(\alpha, Re, M_\infty)$$

The power of the aerodynamic coefficients is further emphasized since dynamic similarity is the very essence of practical wind tunnel testing.

II. METHODOLOGY AND APPROACH

Performance assessment of the aerodynamic behaviour of NACA 64A212 airfoil was based on the numerical approach using the following tools:

- Geometrical/Solid modelling tools
- Mesh generation tool
- Computational Fluid Dynamics (CFD) tool

Figure 1 illustrates the approach adopted during the study.

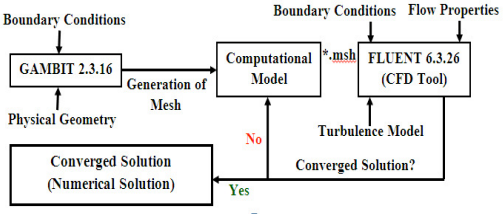

Fig 1. Modelling Approach

The 2-D geometrical model of the airfoil was created in AutoCAD 2012 using its coordinates and then imported to the solid modelling and mesh generation tool, GAMBIT 2.3.16 as shown in figure 2.

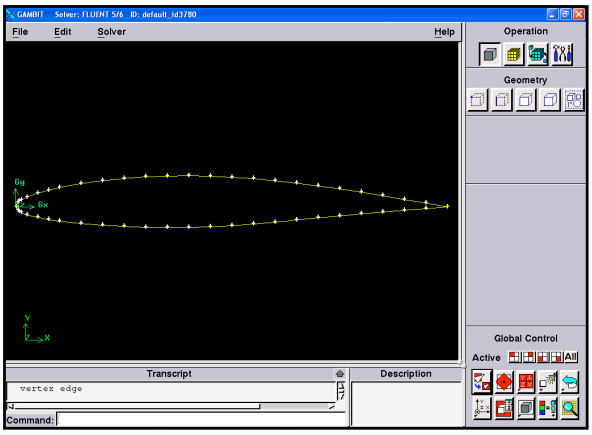

Fig 2. Geometrical model of NACA 64A212 airfoil

A quadrilateral mesh was generated on the computational domain using GAMBIT 2.3.16 for facilitating the solution of flow transport equations. The resolution of the mesh was varied in the domain for optimizing the accuracy of the solution and to compromise with the computational time. On this basis, a finer mesh was established adjacent to the airfoil to facilitate the computation of radical changes taking place due to boundary layer interactions and viscous effects. Areas of the computational domain, where the changes in the flow behaviour are not substantial were incorporated with a coarse mesh as shown in figure 3.

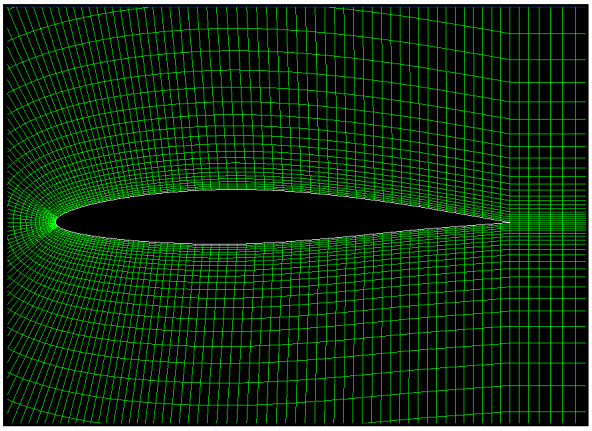

Fig 3. Computational mesh around airfoil

The computational model was imported to *Ansys Fluent 6.3.26,* a commercial CFD tool used as the simulation engine during the study. Spalart-Allmaras model was used for modelling turbulence since it is widely accepted as a typical model for aerodynamic applications. All related boundary conditions and flow physics were also incorporated in the model. Simulations were run on a 3.2 GHz workstation of 4.0 GB RAM at the Faculty of Engineering of the General Sir John Kotelawala Defence University, Sri Lanka until the solution converged, as shown in figure 4. The process was repeated for all related Mach numbers and angles of attack.

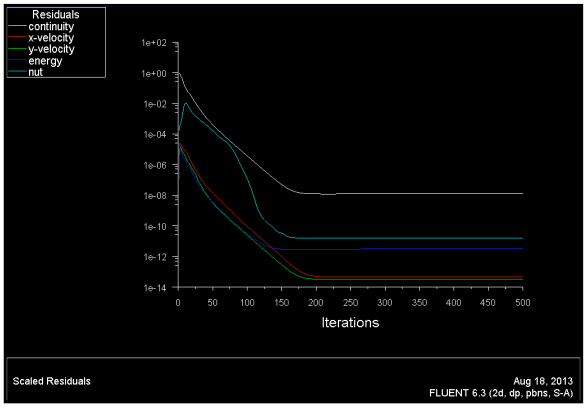

Fig 4. Solution reaching the state of convergence

III. Results and Discussion

At subsonic speeds the progressive increment in M_∞ M_∞ results in a proportional increment in $c_l c_l$, and this can be associated with the fact that lift is created mainly due to the pressure distribution on the surface. As M_∞ M_∞ increases, so does the compressibility effects, which makes profound changes in pressure at different points on the surface as depicted in Figure 5. The oscillatory variation of $c_l c_l$ near Mach 1 is a typical illustration of the transonic shock wave-boundary layer interaction. This phenomena which is a prominent transonic effect, causes upstream pressure propagation at the shock base through the relatively stagnant boundary layer thereby quickening separation or separation. The effect is seen as a fluctuation of lift force in the main flow.

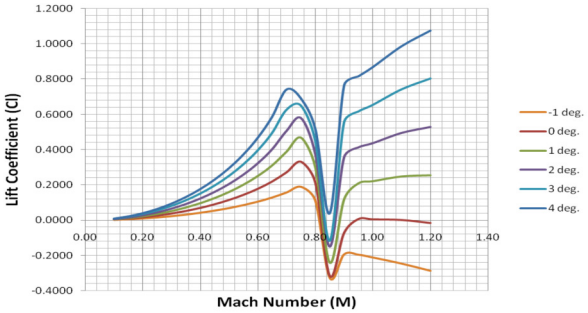

Fig 5. Lift Coefficient vs. Mach Number

The rise in dynamic pressure simultaneously gives rise to drag as shown in figure 6.

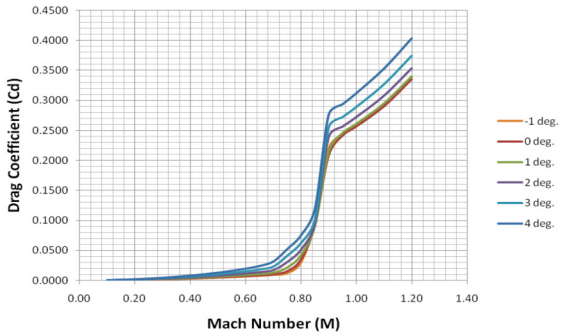

Fig 6. Drag Coefficient vs. Mach Number

Subsonic drag remains constant and relatively small since skin friction is the main source of drag at low speeds. In fact the decrease in skin friction drag coefficient ($c_f c_f$), as $M_\infty M_\infty$ increases can be ignored since the effect is relatively small. In the subsonic regime, drag coefficient is labeled as profile drag coefficient, which stems from skin friction drag and pressure drag due to flow separation($c_{d,p}$), also known as form drag. In coefficient form we have,

$$c_d = c_f + c_{d,p}$$

For a relatively thin airfoil, a close approximation for $c_f c_f$ is obtained through results for a flat plate in incompressible flow:

$$c_f = \frac{1.328}{\sqrt{Re}}$$

where Re is the Reynolds number. However, no such exact theoretical results for turbulent flow exist; rather there are various empirical flat plate formulas for incompressible turbulent flow, as shown below[1]: The calculation of c_f must be done implicitly.

$$(c_d)^{-1/2} = 4.13\log(\mathrm{Re}\, c_f)$$

The flow over the airfoil remains smooth and attached until the Critical Mach ($M_{crit} M_{crit}$) number is reached. As the incipient shocks form at the top and bottom surfaces of the airfoil, thereby inducing separation, pressure drag becomes prominent. This is caused when the integrated pressure distribution over the airfoil becomes unbalanced between the front and rear parts, producing a net drag force. This is further worsened as the shock wave interacts with the boundary layer. It is seen that the drag divergence occurs somewhere around $M_\infty M_\infty$=0.85.

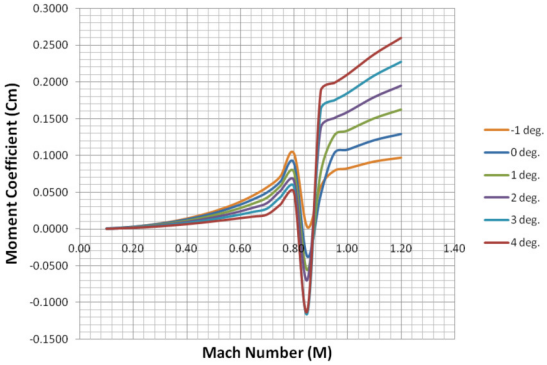

Fig 7. Moment Coefficient vs. Mach Number

The variation of moment shown in figure 7 is mainly due to pressure distribution over the body and qualitatively resembles the variation of the drag coefficient as shown in figure 6.

[1] Karman-Schoenherr curve for variation of incompressible turbulent skin-friction coefficient for a flat plate as a function of Reynolds number.

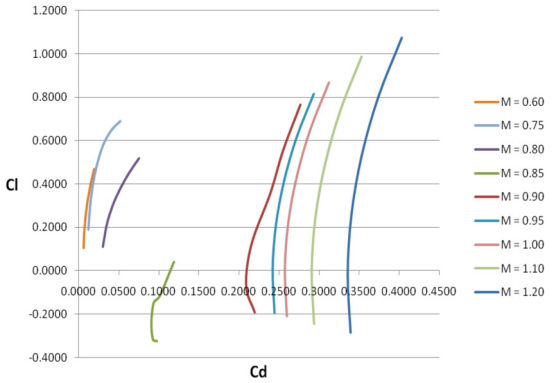

Fig 8. Drag Polar

The Drag polar, a graphical representation of all aerodynamic information necessary to conduct a performance analysis of an aircraft, is drawn for the subsonic and transonic region in figure 8. Each point in the drag polar corresponds to different angles of attack of the airplane. The tangent line to the drag polar drawn from the origin locates the point of maximum lift-to-drag ratio for the airplane. The associated angle of attack represents the angle of attack the airplane must fly at$(L/D)_{max}$ $(L/D)_{max}$. This is called the design point of the aircraft. The variation in the design point of the aircraft is shown as a function of the Mach number in figure 9.

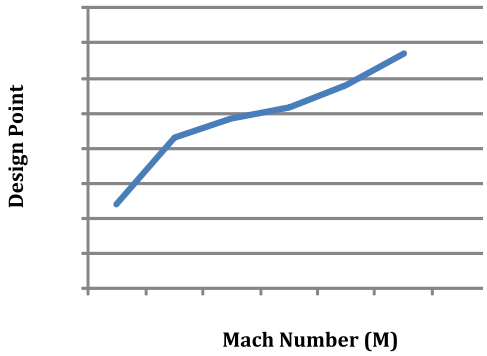

Fig 9. Variation of Design point with Mach Number

The maximum lift-to-drag ratio does not correspond to the minimum drag of the aircraft. When an airplane pitches to its zero-lift angle of attack, the parasite drag becomes slightly higher than the minimal value. Thus the drag polar is represented by the following equation:

$$C_D = C_{D_{min}} + K(C_L - C_{L_{\text{min drag}}})^2$$

The difference between $C_{D,0}$ $C_{D,0}$ and $C_{D\,min}$ $C_{D\,min}$ is infinitesimal for moderate cambered airfoils. Thus the above equation can be treated as the analytical equation for the drag polar:

$$C_D = C_{D,0} + KC_L^2$$

where the minimum drag coefficient is replaced by the zero-lift parasite drag coefficient.

The drag polar for a given airfoil will change depending on the free stream Mach number. At low subsonic speeds the differences will be small and can be ignored. However as speed increases, especially above the critical Mach number, and compressible effects become more prominent, the differences are larger.

Increase encountered in drag in the transonic regime translates the entire drag polar to the right, thus justifying the increase in $C_{D_{min}}$ $C_{D_{min}}$ due to the effects of drag divergence.

The velocity magnitude profile in figure 10 shows the sudden retardation in flow due to the presence of the shock waves in the top and bottom surfaces as well as the stagnation areas in the leading and trailing edges and in the boundary layer. The static pressure profile in figure 11 validates the results obtained through intuition for an infinite two dimensional airfoil in subsonic and transonic regimes.

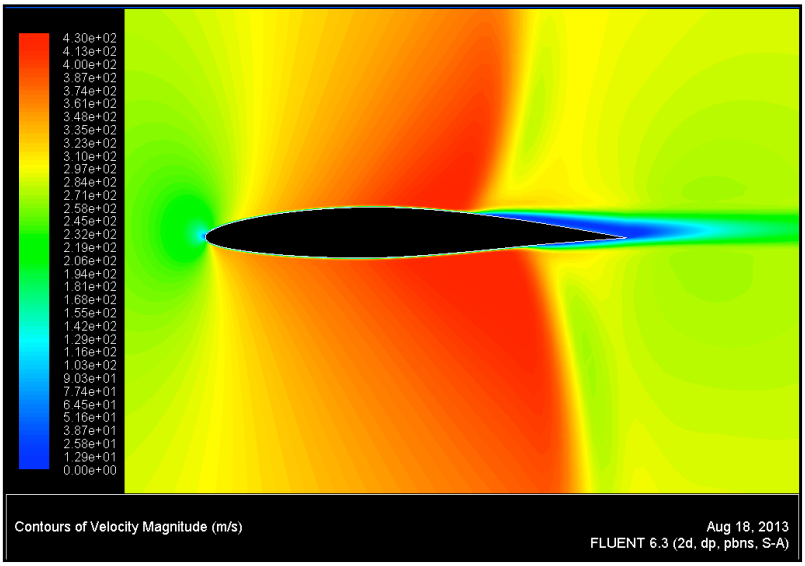

Fig 10. Velocity Magnitude profile

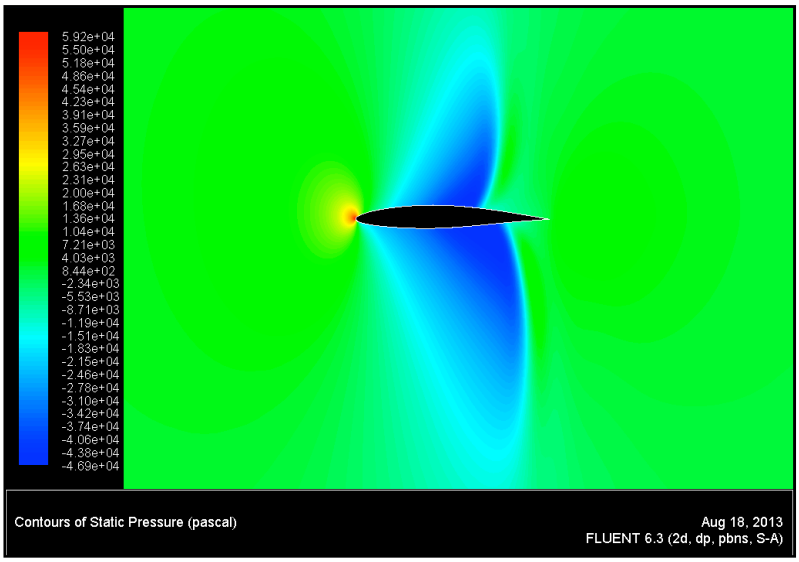

Fig 11. Static Pressure profile

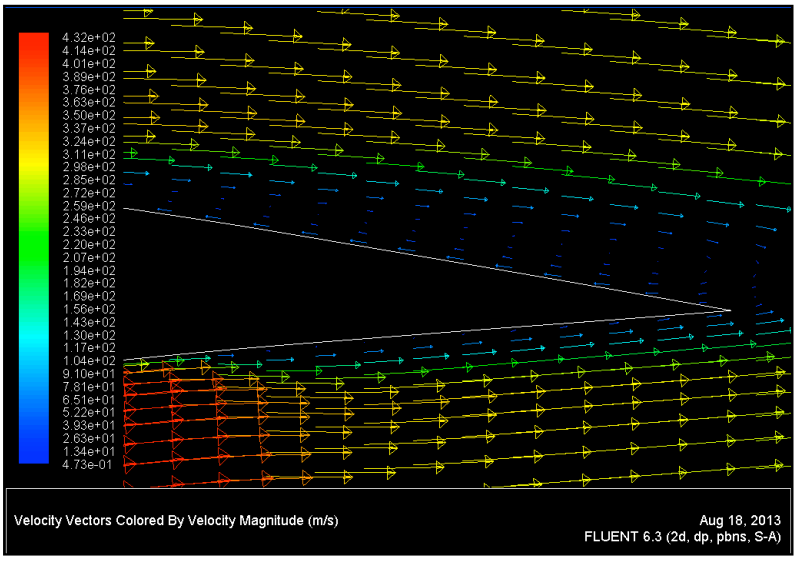

Fig 12. Velocity Vector profile

The velocity vectors in the trailing edge are closely inspected in figure 12. Fluid elements are not only retarded due to skin friction, but also have to work their way against the adverse pressure gradient. This causes flow separation creating a large wake of re-circulating flow down-stream. The effective area producing lift is now destroyed which results in a rapid loss of lift and in turn the coefficient.

IV. CONCLUSION

A preliminary performance analysis of the two-dimensional, infinite NACA 64A212 airfoil has been conducted during present work. Vital information regarding the flow physics unique to the particular airfoil, most prominently the drag polar was generated. The subsonic and transonic behaviour was analyzed in terms of lift, drag and moment coefficients. The generated data will serve as a base for future research in modelling wings with similar wingtips as well as analyzing the performance of wing-body combinations of real aircraft. Wind tunnel experiments with flow visualization and solid data acquisition techniques will assist in model improvement and validation of generated data.

REFERENCES

Anderson Jr JD (2010). Aircraft Performance, McGraw-Hill.

Anderson Jr JD (2011). Fundamentals of Aerodynamics, McGraw-Hill.

Carmichael R (2010). 6A – Series Sections, Available: http://www.pdas.com/sections6a.html [Accessed 10 Feb 2013].

FLUENT 6.3 User's Guide (2006), Fluent Inc.

Tu J Yeoh GH and Liu C (2008). Computational Fluid Dynamics – A Practical Approach, Buttcmurth-Heincmnn publications, UK.

BIOGRAPHY OF AUTHORS

[1]Author is a senior lecturer of Mechanical Engineering at General Sir John Kotelawala Defence University (KDU), Sri Lanka. His research interests include Computational Modelling and Optimization of Energy Systems. At present he holds the position of Head of Department of Mechanical Engineering at KDU. He has 15 years of both academic and industrial experience. His teaching areas include Thermodynamics, Heat and Mass Transfer and Computational Fluid Dynamics.

[2]Author, Sqn Ldr JI Abeygoonewardena is a senior lecturer of Aeronautical Engineering at General Sir John Kotelawala Defence University (KDU), Sri Lanka. Her research interests include Flight Dynamics and Cooperative and Autonomous Behaviour of Unmanned Aerial Vehicles. She has been in active service in the Sri Lanka Air Force as an Aeronautical Engineer for the past 15 years. Her teaching areas include Aerodynamics, Aircraft Stability & Control and Air breathing Propulsion.